We thank the members of the electron-scattering group at Stanford Linear Accelerator Center (see Ref. 3) for discussions of their data before publication.

*Work supported by the U. S. Atomic Energy Commission.

[1]T. T. Wu and C. N. Yang, Phys. Rev. 137, B708 (1965). A discussion of how such a connection might arise in the quark model has been given by J. J. J. Kokkedee and L. Van Hove, Nuovo Cimento 42A, 711 (1966); L. Van Hove, in Lectures at 1966 Scottish Universities Summer School in Physics, edited by T. Preist and L. Vick (Oliver and Boyd Publishers, London, England, 1967). See also H. Schopper, CERN Report No. CERN 67-3, 1967 (unpublished).

[2]G. Cocconi et al., Phys. Rev. 138, B165 (1965); J. V. Allaby et al., Phys. Letters 23, 389 (1966); J. V. Allaby et al., Phys. Letters 25B, 156 (1967).

[3]D. H. Coward et al., Phys. Rev. Letters 20, 292 (1968) (this issue).

[4]J. Orear, Phys. Letters 13, 190 (1964).

[5]A. D. Krisch, Phys. Rev. Letters 19, 1149 (1967).

[6]An especially inspirational passage on this idea has been given by R. P. Feynman, in Proceedings of the Thirteenth International Conference on High Energy Physics, Berkeley, 1966 (University of California Press, Berkeley, California, 1967), p. 98.

[7]The data of A. M. Boyarski et al., Phys. Rev. Letters 20, 300 (1967) (this issue), strongly indicate that one may be a bit hasty in including the pion among "other known trajectories."

[8]At this point the isotopic and unitary spin properties of the current in the contact interaction are not specified beyond saying that its diagonal matrix element in the proton state exists.

[9]Specifically we mean the form factors $F_1(t)$ and $g_A(t)$ which are the coefficients of γ_α and $\gamma_\alpha\gamma_5$, respectively. If the scaling law $G_{Ep}(t)=G_{Mp}(t)/G_{Mp}(0)$ holds, as assumed by Coward et al., Ref. 3, then $F_{1p}(t)$ becomes proportional to $G_{Mp}(t)$ for large t.

[10]With $a=1$ our conjectured form for $d\sigma/dt$ if applicable at $t=0$, which we specifically do not propose, leads to equal real and imaginary amplitudes in conflict with experiment. Among the many arguments against applying our considerations elsewhere than in the region of large s and $-t$ is the observation that iterations of the contact interaction at small t lead to increasing contributions from higher order terms containing at least logs.

[11]For the Regge model one may consult D. H. Sharp and W. G. Wagner, Phys. Rev. 131, 2227 (1963).

[12]The observation that the 30-BeV p-p data already reveal the asymptotic behavior of the optical model for large s has been made earlier by Serber in analyzing the t dependence of the data in Ref. 2. See R. Serber, Rev. Mod. Phys. 36, 649 (1964).

ZERO-DEGREE PRODUCTION OF HIGH-MOMENTUM π^+ MESONS BY π^- MESONS INCIDENT ON NUCLEI*

R. A. Lundy, I. A. Pless,† D. R. Rust, and D. D. Yovanovitch
Argonne National Laboratory, Argonne, Illinois

and

Vera Kistiakowsky
Massachusetts Institute of Technology, Cambridge, Massachusetts

(Received 18 December 1967)

We have studied π^+ production at 0° by 2- to 6-BeV/c π^- incident on beryllium, carbon, copper, lead, and polyethylene. The experiment was done in the 17° negative pion beam at the zero-gradient synchrotron (ZGS) at Argonne National Laboratory.

The experimental setup is shown in Fig. 1. The arrangement consists of a two-stage beam spectrometer followed by a detection system. The first section of the spectrometer uses the fringe field of the ZGS followed by a system of two quadrupoles and a bending magnet. A momentum slit is placed at the focus of this first section. The second section is a symmetric system consisting of four quadrupoles and a bending magnet. Our target material was placed just after the momentum slit, a choice dictated by the physical arrangement of the

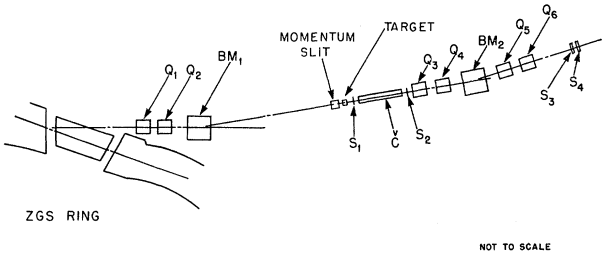

FIG. 1. The ZGS 17° beam. The π^- of the desired momentum were focused on the momentum slit by quadrupoles Q_1 and Q_2 and bending magnet BM_1. Q_3, Q_4, BM_2, Q_5, and Q_6 were tuned to select π^+ of given momenta from the target.

counters and the existing beam. The second section was tuned to positive particles so that the momentum slit was imaged on the last two counters of the detection system. This arrangement produced considerable background from the slit itself; hence the slit subtraction was large and was a limiting factor in these measurements.

The first momentum slit defines a momentum acceptance of 1.4% (full width at half-height). The momentum resolution of the second section was also 1.4% (full width at half-height). Measurements were made by tuning both arms of the spectrometer for a given π^- momentum. Then all the currents in the second half of the spectrometer were reversed so that this section accepted only positive particles. It was varied through a wide range of positive momentum values during the experiment. The solid angle of the second spectrometer was 3×10^{-4} sr.

The detection system consisted of four counters ($S_1S_2S_3S_4$) in coincidence. A Cherenkov counter after the momentum slit enabled us to determine the composition of the positive beam. During the run, the Cherenkov counter was set to detect e^+ and placed in anticoincidence with the four counters.

There are several possible mechanisms for producing positive pions in complex nuclei. One is double charge exchange:

$$\pi^- + (Z,A) \rightarrow \pi^+ + (Z-2,A). \quad (1)$$

A second mechanism is direct π^+ production on a nucleon bound in the nucleus:

$$\pi^- + p \rightarrow \pi^- + \pi^+ + n. \quad (2)$$

A third is the production of a single nucleon

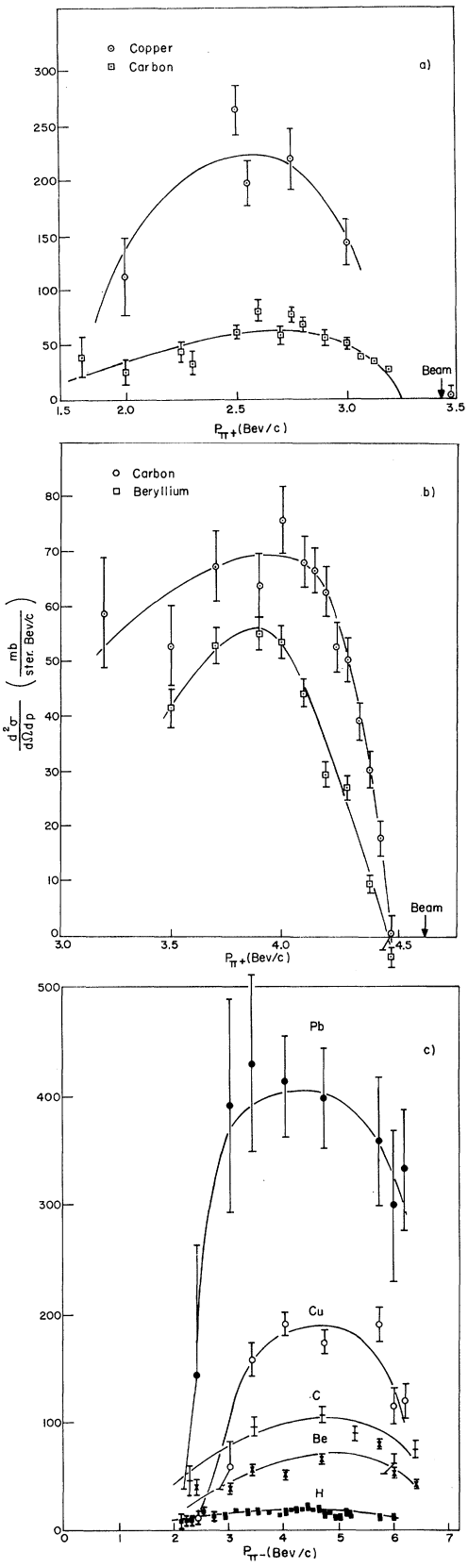

FIG. 2. (a) Momentum spectrum of π^+ produced at 0° by π^- of 3.47-BeV/c (nominal) momentum incident on copper and carbon. (Nominal momentum means the spectrometer setting uncorrected for hysteresis.) (b) Momentum spectrum of π^+ produced at 0° by π^- of 4.70-BeV/c (nominal) momentum incident on carbon and beryllium. (c) Excitation curve of π^+ produced at 0° by π^- incident on hydrogen, beryllium, carbon, copper, and lead. The momentum at which the π^+ were measured was 300 MeV/c lower than the incoming π^- momentum (nominal) in the case of hydrogen. For all other elements, the momentum at which the π^+ were measured was 800 MeV/c lower than the incoming π^- momentum (nominal).

resonance inside the nucleus:

$$\pi^- + p \rightarrow N^{*-} + \pi^+. \quad (3)$$

A fourth mechanism is the production of a boson that then decays into pions:

$$\pi^- + p \rightarrow X^0 + n, \quad X^0 \rightarrow \pi^+ + \pi^-. \quad (4)$$

In principle, one can distinguish between these processes at 0° by measuring the peak momentum of the emerging π^+. In Reaction (1) the peak energy is essentially the incident beam energy, while in Reaction (2) the cross section rises slowly from a maximum energy which is approximately a pion mass less than that of the incident beam. In Reaction (3), a peak in the momentum spectrum would be expected at a position corresponding to the missing mass of an N^{*-}. The distinguishing features of Reaction (4) depend in a very sensitive way on both the production and decay angular distribution of the X^0, but the maximum momentum of the π^+ would be significantly less than the incoming momentum.

The second section of the spectrometer was usually set for positive particles and was reversed only when it was necessary to change the momentum of the first section, since the calibration of the first section was done by the second. Therefore, there could be a hysteresis effect in the calibration of the incoming π^- beam momentum. We estimate that this hysteresis effect could result in a nominal momentum about 50 MeV/c greater than the real value of the π^- momentum. The arrows in Fig. 1 indicate our best knowledge of the π^- beam momentum.

Figure 2(a) shows the π^+ spectrum from beryllium and copper for an incident π^- beam of nominal momentum 3.47 BeV/c. Figure 2(b) shows the spectrum for carbon and copper for an incident π^- beam of nominal momentum 4.70 BeV/c. There are two striking features about the curves in Figs. 2(a) and 2(b). The first is the absence, within our statistical uncertainty, of π^+ mesons near the momentum of the incoming π^- beam. The second is the very sharp increase in the production of π^+ mesons about 150 MeV below the momentum of the incoming π^- beam. The implications of these features are the following: (a) Double charge exchange (mechanism 1) is not the dominant mechanism for producing π^+ mesons at 0°; (2) direct production (mechanism 2) also seems to be ruled out by the sharp rise. Either single-nucleon resonance or boson production probably is occurring inside the nucleus. In the first case (mechanism 3), the π^+ are probably produced in conjunction with a resonant state of a quasifree nucleon inside the nucleus; in the second (mechanism 4), a neutral boson is produced which decays to the π^+ and a π^-.

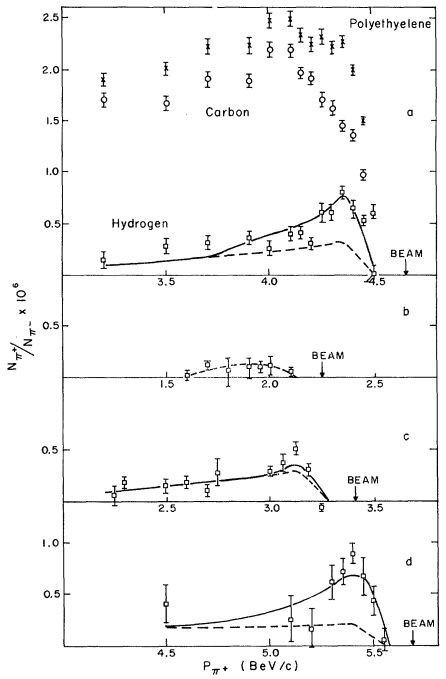

FIG. 3. (a) Momentum spectrum of π^+ produced at 0° by π^- of 4.7-BeV/c (nominal) momentum incident on hydrogen. Also shown are the polyethylene and carbon data. The solid curve is a Monte Carlo prediction assuming f^0 and ρ^0 production. The dashed curve is the prediction of the Monte Carlo for the ρ^0 production alone. (Nominal momentum means the spectrometer setting uncorrected for hysteresis.) (b) Momentum spectrum of π^+ produced at 0° by π^- of 2.3-BeV/c (nominal) momentum incident on hydrogen. The curve is the Monte Carlo prediction. (c) Same as (b) but for 3.47-BeV/c (nominal) incoming π^- momentum. (d) Same as (b), but for 5.74-BeV/c (nominal) incoming π^- momentum.

The possibility of resonance or boson production in hydrogen was explored by the polyethylene-carbon difference method. Figure 3(a) shows the π^+ spectrum from hydrogen at 4.7 BeV/c. The carbon and polyethylene data are shown, as well as the subtraction. Figures 3(b)-3(d) show the π^+ spectrum from hydrogen at 2.3, 3.47, and 5.74 BeV/c, respec-

tively. These curves have some striking features in common. The first is that the π^+ production rises sharply some 150 MeV below the incident momentum. The second is that there is a peak in the cross section some 250 MeV below the incident π^- momentum. The third common feature is a presence of a broad peak or shoulder of π^+ mesons at lower momenta. Note that the 2.3-BeV/c data do not have the pronounced high-momentum peak.

For all momenta, the center of the high-momentum peak in Fig. 3 corresponds to a missing mass of approximately 1.2 BeV. If the nominal value of the incident π^- momentum is used, a missing mass of nearly 1.24 BeV is calculated for all momentum. This suggests that the reaction we are observing is the production of the negative member of the familiar (1238) isobar family (mechanism 3). Using the corrected beam momentum, a crude estimate of errors would indicate a central value of 1.2 BeV $\pm$ 50 MeV and a width of 150 $\pm$ 60 MeV for all momenta, except for 2.3 BeV/c, where the high-momentum peak is missing.

However, this is not a unique interpretation of the data. The following reactions are well established:

$$\pi^- + p \rightarrow \rho^0 + n, \quad \rho^0 \rightarrow \pi^+ + \pi^-, \tag{5}$$

$$\pi^- + p \rightarrow f^0 + n, \quad f^0 \rightarrow \pi^+ + \pi^-. \tag{6}$$

For all energies above 3.5 BeV/c, the maximum momentum of the π^+ for Reactions (5) and (6) is about 140 MeV below the incident π^- momentum, in agreement with our observations. We calculated the π^+ momentum spectra to be expected from both Reactions (5) and (6) as observed by our experimental geometry. We used a Monte Carlo program, "N Vertex,"[1] together with the experimental cross sections[2,3] and production angular distributions[2,3] to obtain these results. Calculations were performed for various decay angular distributions for the ρ^0 and the f^0, and although the magnitudes of the detection efficiencies were found to be sensitive to the decay distribution chosen, the shape of the momentum distributions were not. The distributions used in the curves presented in this paper were $[P_2(\cos\theta)]^2$ for the f^0 and $4 + 5\cos^2\theta$ for the ρ^0. The experimental ρ^0 distribution is not symmetric, but our experimental apparatus is totally insensitive to the backward π^+ distribution. The forward shape is represented quite well[3] by $4 + 5\cos^2\theta$, which was used to simplify our programs and shorten our computer running time.

Figure 3 shows the results of these calculations. The solid lines are the calculated spectra for the various incident π^- momenta for the appropriate combination of f^0 and ρ^0 production. Since there is a considerable systematic uncertainty, the curves have been normalized to the data. However, the normalization factor is consistent with 1 for all incoming momenta within the systematic uncertainties. The shapes of the calculated curves are in agreement with the data within the statistical uncertainties. Since the threshold for f^0 production is about 2.1 BeV/c, the curve calculated for an incoming π^- momentum of 2.3 BeV/c does not have a high-momentum peak. The experimental data are in agreement with the absence of such a peak.

As previously stated, these data seem to be in agreement with the predictions of mechanisms 5 and 6, but not with those of mechanisms 1 and 2. However, this experiment cannot conclusively determine the mechanism for the observed production of π^+ by π^-. The possibility of N^{*-} production (mechanism 3) cannot be ruled out. Nevertheless, these data can be fitted very well by assuming that ρ^0 and f^0 production (mechanism 4) alone contribute. In particular, the disappearance of the high-momentum peak near f^0 threshold seems a strong indication that f^0 production is a mechanism involved.

Figure 2(c) shows the differential cross sections for the production of π^+ by π^- incident on hydrogen, beryllium, carbon, copper, and lead. Except for hydrogen, the measurements were made for a π^+ momentum 800 MeV/c below the π^- nominal beam momentum. For hydrogen, the measurements were made for a π^+ momentum 300 MeV/c below that of the π^- beam. Above 3.5 BeV/c the production as a function of A goes roughly as $A^{1/3}$. All cross sections seem to rise to about 5 BeV/c, and then start to fall. This general behavior seems to follow the pattern of the f^0 production cross section.

It is interesting to note that the cross section per nucleon for the production of π^+ by π^- on beryllium is comparable with that for producing π^+ by protons on beryllium.[4]

All points in Figs. 2 and 3 are corrected for absorption in the targets. (The beryllium target was 8 in. long, the carbon target was 5 in.

long, the copper target was 3 in. long, the lead target was 2 in. long, and the polyethylene target was 11 in. long. This corresponds to 36 g/cm^2 of beryllium, 23 g/cm^2 of carbon, 68 g/cm^2 of copper, 58 g/cm^2 of lead, and 27 g/cm^2 of polyethylene.) There is a combined systematic uncertainty of about 30% in our solid angle and resolution. Hence all cross sections have a systematic uncertainty of 30%.

A measurement of the contamination of the π^- beams produced at 3.47 BeV/c indicated less than 20% contamination by protons and K^+. At 5.0 and 5.3 BeV/c there was no contamination within the 7% statistical uncertainties. During this run we had 10^6 π^- per ZGS pulse at 4.70 BeV/c. This incident flux produced 10 π^+ mesons at 4 BeV/c and 0° from our beryllium target, a beam suitable both in intensity and purity for a bubble chamber.

We wish to thank the staff of the ZGS for the aid and cooperation which made this experiment possible. In addition, we would like to thank Professor V. L. Teplitz and Professor M. Ross for valuable discussions.

*Work supported in part through funds provided by the U. S. Atomic Energy Commission.

†Permanent address: Massachusetts Institute of Technology, Cambridge, Mass. 02139.

[1]C. A. Bordner, Jr., A. E. Brenner, and E. E. Ronat, Rev. Sci Instr. 37, 36 (1966).

[2]D. R. Clear et al., Nuovo Cimento 49A, 399 (1967); Y. Y. Lee et al., Phys. Rev. 159, 1156 (1967); D. H. Miller et al., Phys. Rev. 153, 1423 (1967); E. West et al., Phys. Rev. 149, 1089 (1966); V. Hagopian et al., Phys. Rev. 145, 1128 (1966); J. P. Baton et al., Nuovo Cimento 35, 713 (1965); Saclay-Orsay-Bari-Bologna Collaboration, Nuovo Cimento 29, 3625 (1963); J. J. Veillet et al., Phys. Rev. Letters 10, 29 (1963); L. Bondar et al., Phys. Letters 5, 153 (1963).

[3]R. L. Eisner et al., Phys. Rev. 164, 1699 (1967).

[4]R. A. Lundy et al., Phys. Rev. Letters 14, 504 (1965).

MEASUREMENT OF THE ENERGY DEPENDENCE OF THE FORM FACTOR IN $K_L^0 \to \pi + e + \nu$ DECAY*

Samuel H. Aronson† and K. Wendell Chen

Palmer Physical Laboratory, Princeton University, Princeton, New Jersey

(Received 27 September 1967)

The pion energy distribution in $K_L^0 \to \pi + e + \nu$ decay has been measured at the Princeton-Pennsylvania Accelerator using a wide-gap spark-chamber spectrometer. The results are consistent with vector interaction and an energy-independent form factor. The energy-dependence parameter λ is found to be $+0.020 \pm 0.013$.

The $|\Delta I| = \frac{1}{2}$ rule in semileptonic weak interactions predicts that the vector form factor f_+ should exhibit the same dependence on pion energy in both $K^+ \to \pi^0 + e^+ + \nu$ (K_{e3}^+) and $K_L^0 \to \pi^\pm + e^\mp + \nu$ (K_{e3}^0) decays.[1] Experiments on K^+ decays have found no evidence of variation of f_+ with pion energy.[2] On the other hand, published experiments on K_L^0 decays have obtained conflicting results.[3] Three of the previous experiments found some energy dependence, but their errors were large; the most recent experiments are consistent with no energy dependence. We report here briefly on a spark-chamber experiment which was undertaken to obtain further information on the energy dependence of f_+ in K_{e3}^0 decay.

The source of K_L^0 mesons was the 13° neutral beam at the Princeton-Pennsylvania Accelerator (PPA). The beam was collimated and passed through 10 radiation lengths of lead to reduce its gamma-ray component. Charged particles were removed by a series of sweeping magnets and collimators. The radio-frequency structure of the PPA beam permitted measurement of the time of flight of the K_L^0 mesons, an advantage absent in other similar experiments.[3] This information was used to eliminate the twofold kinematical ambiguity which arises in reconstructing the K_L^0 momentum. The K_L^0 detector was a thin-electrode, wide-gap spark chamber consisting of two $17\frac{1}{2}$-in. gaps placed in a 36-in. spark-chamber magnet. The magnetic field was 6 kG. A detailed description of the wide-gap spark chamber has been presented elsewhere.[4] The chamber was triggered by two charged particles passing through any two of four scintillation-counter telescopes arranged around the beam downstream from the chamber. Each telescope contained a lead-Lucite Cherenkov shower counter[5] for